Applied Physics Letters

Electrochemical control and protonation of the strontium iron oxide $SrFeO_y$ by using proton-conducting electrolyte

Cite as: Appl. Phys. Lett. **120**, 091601 (2022); https://doi.org/10.1063/5.0083209
Submitted: 22 December 2021 • Accepted: 17 February 2022 • Published Online: 01 March 2022

Yosuke Isoda, Daisuke Kan, Yumie Ogura, et al.

Applied Physics Letters ARTICLE scitation.org/journal/apl

Electrochemical control and protonation of the strontium iron oxide $SrFeO_y$ by using proton-conducting electrolyte

Cite as: Appl. Phys. Lett. **120**, 091601 (2022); doi: 10.1063/5.0083209
Submitted: 22 December 2021 · Accepted: 17 February 2022 ·
Published Online: 1 March 2022

Yosuke Isoda,[1] Daisuke Kan,[1,a)] Yumie Ogura,[2] Takuya Majima,[2] Takashi Tsuchiya,[3] and Yuichi Shimakawa[1]

AFFILIATIONS

[1]Institute for Chemical Research, Kyoto University, Uji, Kyoto 611-0011, Japan
[2]Department of Nuclear Engineering, Kyoto University, Kyoto 615-8540, Japan
[3]International Center for Materials Nanoarchitectonics (WPI-MANA), National Institute for Materials Science (NIMS), Tsukuba, Ibaraki, Japan

[a)]Author to whom correspondence should be addressed: dkan@scl.kyoto-u.ac.jp

ABSTRACT

To electrochemically control structural and transport properties of oxygen-deficient perovskite $SrFeO_y$ ($2.5 \leqq y \leqq 3$) (SFO) epitaxial films, we employed electric-field-effect transistor structures in which the proton-conducting solid electrolyte Nafion is used as a gate insulator. When a positive gate voltage (V_{GS}) is applied and protons are injected toward the film channel layer, the SFO films are electrochemically reduced, leading to increases in the channel resistance. On the other hand, when a negative V_{GS} is applied and protons are removed, the SFO films are oxidized, and as a result, the channel resistances decrease. In addition, we found that the electrochemically reduced SFO films accommodate protons, forming the proton-containing oxide $H_xSrFeO_{2.5}$ whose proton concentration is determined by elastic recoil detection analysis to be $x \sim 0.11$. Our results indicate the usefulness of the proton-conducting solid electrolyte for electrochemically controlling transition metal oxides and for exploring proton-containing oxides.

Various structural and physical properties of transition metal oxides are closely tied to their valence states.[1] Therefore, utilizing electrochemical redox reactions and modulating transition metals' valence states enable one to electrically control oxides. Fabricating electric-field-effect transistor structures having gate insulators of electrolytes is found to be a way for electrically inducing redox reactions in channels of oxide films and for electrochemically controlling oxides' physical properties.[2–10] Regardless of forms of electrolytes (liquid or solid), water molecules (or protons) contained in electrolytes have been considered to play a key role in field-induced redox reactions in transistor structures. Recently, it was also shown that the electrochemically reduced oxygen-deficient oxides can accommodate protons, leading to a transformation of oxides to proton-accumulated materials.[11–13] An important implication is that utilizing proton-conducting electrolytes as gate insulators in transistor structures is useful for electrically controlling oxides and for exploring proton-containing materials that have not been synthesized by conventional solid-state reactions.

In the work reported here, we used the proton-conducting solid electrolyte Nafion, which contains a large amount of water and protons, as a gate insulator and demonstrated electrochemical control and protonation of oxygen-deficient iron oxide $SrFeO_y$ (SFO). Structural and electrical transport properties of SFO are known to depend on oxygen concentration y that ties with the Fe valence state (or the carrier density).[14–25] When SFO is oxidized and y is close to 3, the oxygenated SFO ($SrFeO_3$) containing Fe^{4+} exhibits metallic transport properties with low electrical resistivity. On the other hand, when oxygen vacancies are introduced and y is lowered to 2.5, SFO is transformed to the insulating brownmillerite $SrFeO_{2.5}$ containing only Fe^{3+}. Given that SFO is integrated as a channel layer in transistor structures having a gate insulator of Nafion, as shown in Fig. 1(a), electrical properties of the SFO channels are expected to be controlled by electrochemical redox reactions. When a positive gate bias V_{GS} is applied, protons are injected into the channel, and the SFO layers would be electrochemically reduced. When a negative V_{GS} is applied, protons are removed from the channel, and the SFO layers are

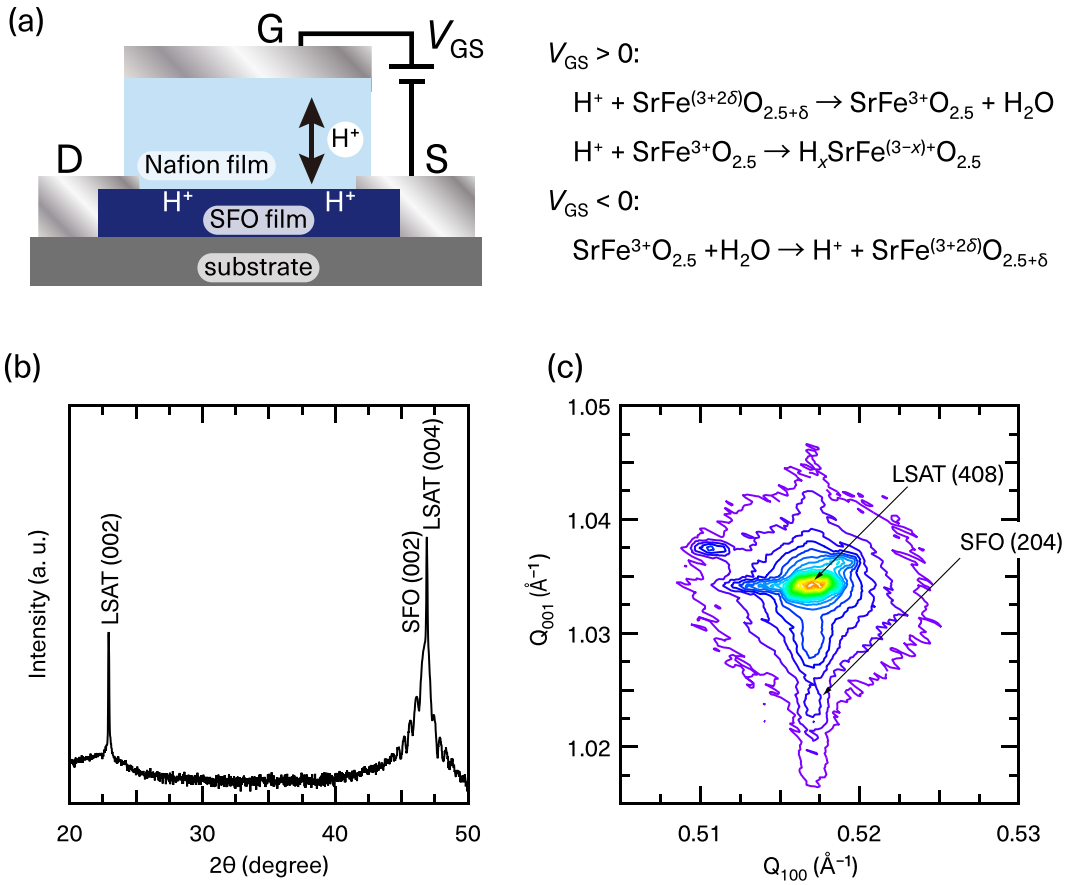

FIG. 1. (a) Schematic illustration of electrochemical transistor device in which the proton-conducting solid electrolyte Nafion is used as a gate insulator. When a positive bias V_{GS} is applied, protons would be injected into the channel and the SFO layers would be electrochemically reduced, resulting in a decrease in carrier density and an increase in electrical resistance. When a negative V_{GS} is applied, protons would be removed from the channel and the SFO layers would be oxidized, leading to an increase in carrier density and a decrease in electrical resistance. (b) X-ray $2\theta/\theta$ diffraction pattern and (c) reciprocal space mapping around the (408) LSAT reflection for the 20 nm thick SFO films epitaxially grown on LSAT substrates.

expected to be oxidized. In fact, as we expected, we show that fabricating transistor structures with Nafion as a gate insulator and applying electric-field redox reactions to SFO film channels enables nonvolatile and reversible control of channels' resistance. Furthermore, electrochemically reducing the channels is found to implant protons into SFO, leading to formation of proton-accumulated oxide $H_xSrFeO_{2.5}$ that has not been seen so far.

SFO epitaxial thin films were prepared on $(LaAlO_3)_{0.3}(SrAl_{0.5}Ta_{0.5}O_3)_{0.7}$ (LSAT) (100) single crystal substrates by pulsed laser deposition (PLD). SFO layers of 20 nm thick were deposited at the substrate temperature of 650 °C and under an oxygen pressure of 50 mTorr. Figures 1(b) and 1(c), respectively, show an x-ray $2\theta/\theta$ pattern and a reciprocal space mapping around the LSAT (408) reflection for the $SrFeO_y$ epitaxial thin films. The $2\theta/\theta$ profile confirms that the SFO films are epitaxially grown with the (001) orientation and that no secondary phases are detected. The out-of-plane lattice constant is ~3.88 Å. This lattice constant is shorter than that for brownmillerite-structured films (~4.0 Å) but is longer than that of fully oxygenated SFO ($SrFeO_3$) films on LSAT substrates.[26] These observations imply that our as-grown SFO films are oxygen-deficient perovskite $SrFeO_y$. Furthermore, the reciprocal-space mapping in Fig. 1(c) shows that the in-plane lattice of the films is fixed by that of the substrate and that the oxygen-deficient perovskite SFO layer is coherently grown on the substrate.

To fabricate transistor structures whose channels are SFO films and gate insulators are Nafion, Pt layers (20 nm thick) that serve as source and drain electrodes were first sputtered at room temperature. Then, Nafion films (Nafion 115, Sigma Aldrich) where Pt layers were sputtered on one side were bonded on the SFO channels by compressing them at 100 °C for 10 min.

To characterize transport properties of the SFO channels in the transistor structure, we applied sequences of the gate voltages V_{GS} and the source–drain voltage V_{SD} as described in Fig. 2(a). First, we applied the V_{GS} ranging between −2 and 2 V for given periods (50–300 s), inducing redox reactions in the SFO channels. The channels' resistances R_{SD} were then measured by applying the source–drain voltage V_{SD} of 0.1 V. We note that during the R_{SD} measurements, the V_{GS} is turned off so as to avoid possible contaminations of gate leakage currents in

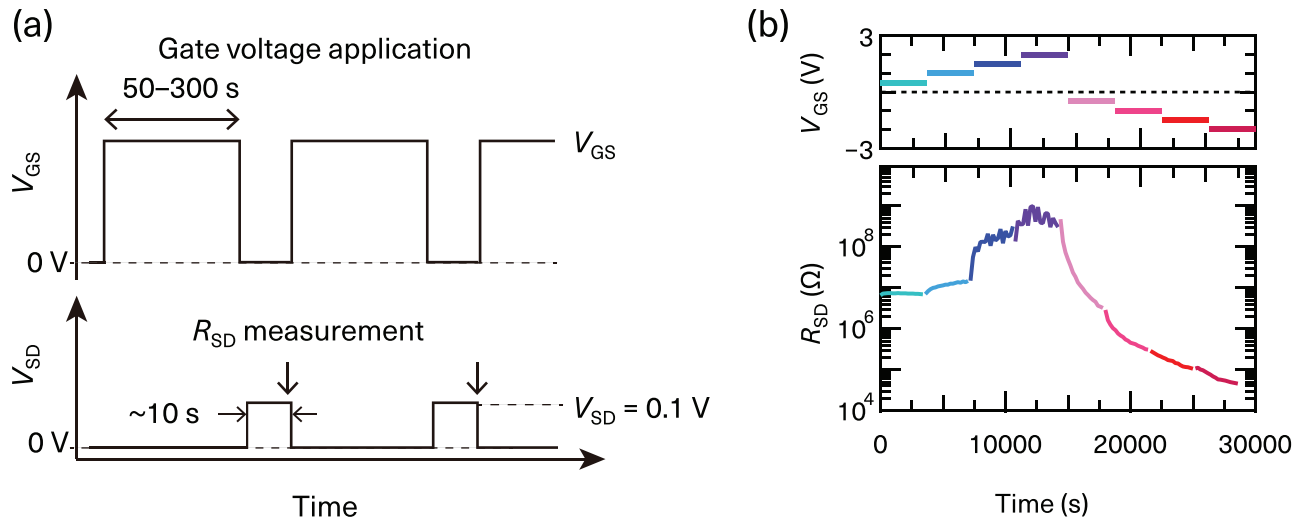

FIG. 2. (a) Voltage sequence used in our measurements. The gate voltage V_{GS} was applied for certain periods (50–300 s), inducing electrochemical redox reactions. Then V_{GS} were turned off and the source–drain voltage V_{SD} of 0.1 V was applied to measure the channel resistance R_{SD}. (b) Gate voltage V_{GS} dependence of the SFO channel resistance R_{SD}. The data were taken for the transistor device whose channel is 1.4 mm wide and 0.8 mm long. The gate leakage currents I_{GS} upon the V_{GS} applications were less than 10^{-5} A. The fluctuations seen in the high R_{SD} region are due to some noise contaminations to the measured currents.

Nafion (about 10^{-6} to 10^{-5} A) to source–drain currents. Figure 2(b) shows the V_{GS} dependence of the R_{SD}. Applying positive and negative V_{GS} are, respectively, found to lead to increases and decreases in R_{SD}. The R_{SD} values measured under $V_{GS} = 0$ V vary depending on the applied V_{GS}. In addition, for the larger $|V_{GS}|$, the R_{SD} becomes almost saturated in shorter periods. These observations indicate that the positive and negative V_{GS} induce reduction and oxidation reactions for the SFO channels, as indicated in Fig. 1(a), and the V_{GS}-induced electrochemical reactions result in the nonvolatile and reversible changes in the R_{SD}. In addition to the electrochemical reactions, V_{GS} applications in a transistor structure might cause electrostatic carrier accumulations into the channel layers. However, electrostatic carrier accumulations would not be at play in our case. Because changes in the channels induced by electrostatic carrier accumulations should be volatile, the R_{SD} measured with our voltage sequences [Fig. 2(a)] should not exhibit any V_{GS} dependence if the carrier accumulation effect were at play.

We also investigated how the V_{GS}-induced redox reactions affect the structural properties of the SFO channels. To this end, we prepared three SFO channels referred to as SFO-A, SFO-B, and SFO-C, respectively, which underwent different sequences of V_{GS} applications. For SFO-A, a Nafion film was thermo-compressed on the as-grown SFO film and then mechanically peeled off without applying V_{GS}. For SFO-B, by applying $V_{GS} = 1.5$ V for one hour in the transistor structure, we electrochemically reduced the SFO channel and then mechanically peeled off the Nafion film. For SFO-C, we first applied $V_{GS} = 1.5$ V for one hour and subsequently $V_{GS} = -1.5$ V for one hour in the transistor structure. After the electrochemical redox reactions, we mechanically peeled off the Nafion film.

Figure 3 shows the $2\theta/\theta$ patterns around the (004) LSAT reflections for SFO-A, SFO-B, and SFO-C. For SFO-B, the (002) SFO reflection slightly shifted to the lower 2θ sides due to electrochemical reductions for the SFO films. In addition, a broad reflection appeared around $2\theta \sim 44.5°$, indicating V_{GS}-induced formation of a crystal lattice whose lattice constant is 4.07 Å. This lattice constant is larger than the lattice constants of bulk $SFO_{2.5}$ and $SrFeO_{2.5}$ films epitaxially strained by LSAT substrates.[26] The appearance of the extra reflection for SFO-B is, thus, considered to result from the protonation of $SrFeO_{2.5}$ films by V_{GS}-induced reduction reactions, which expands the lattice of the $SrFeO_{2.5}$ films. We note that similar lattice expansions

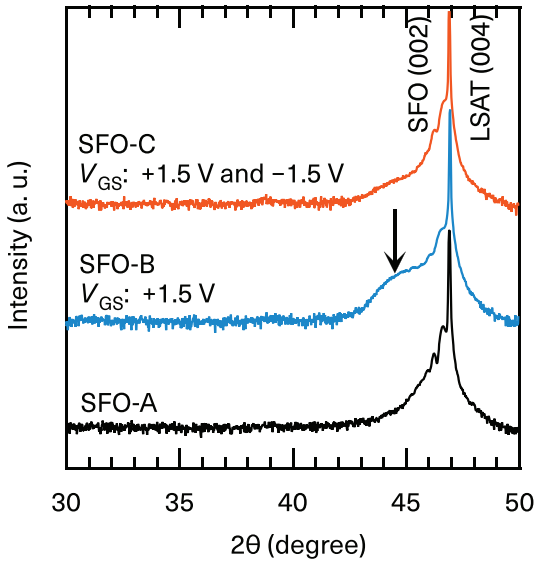

FIG. 3. XRD patterns around the (004) LSAT reflection for SFO films without V_{GS} application (SFO-A), after positive V_{GS} (+1.5 V) application for 1 h (SFO-B) and after positive V_{GS} (+1.5 V) and negative V_{GS} (−1.5 V) applications, each for one hour (SFO-C). For these XRD measurements, SFO channels 5 mm wide and ~3 mm long were used. The broad reflection indicated with the black arrow appears as a result of the V_{GS}-induced protonation of $SrFeO_y$ films.

were also seen when protons were electrochemically introduced to the brownmillerite-structured cobalt oxide $SrCoO_{2.5}$.[11,13] In contrast to the hydrogenated $SrCoO_{2.5}$, no superstructure reflections, such as the (0 0 3/2) reflection characteristic of the c-axis oriented brownmillerite structure, are observed for SFO-B (Fig. 3). This observation might indicate that the hydrogenated $SrFeO_y$ thin films have a brownmillerite structure whose orientation is different from that of the hydrogenated $SrCoO_{2.5}$. In addition, introducing protons to $SrFeO_{2.5}$ might cause large lattice distortions and modify cation arrangements characteristic of the brownmillerite structure. Identifying atomic structures of hydrogenated $SrFeO_y$ films will require further investigations. We also point out that V_{GS}-induced re-oxidation reactions to the electrochemically reduced films (SFO-B) lead to the intensity reduction of the broad reflection around $2\theta \sim 44.5°$, as seen in the diffraction pattern for SFO-C. This observation indicates that electrochemical oxidation reactions lead to deprotonation in the reduced SFO films.

To further confirm the V_{GS}-induced protonation and quantitatively evaluate the hydrogen concentration introduced in SFO films, we carried out elastic recoil detection analysis (ERDA) for SFO-A, SFO-B, and SFO-C films at the 1.7 MV tandem accelerator facility of the Quantum Science and Engineering Center, Kyoto University. The ERDA signals were obtained with 7.5 MeV O^{4+} beams incident at an angle of ~75° to the surface normal and by detecting H atoms recoiling forward from the films at a scattering angle of 30°. The spectra for SFO-A, SFO-B, and SFO-C are shown in Figs. 4(a)–4(c), respectively. The ERDA signal intensities plotted are normalized with Rutherford backscattering spectrometry (RBS) signals for each film. The obtained ERDA spectra were also reproduced by simulation with the SIMNRA 7.03 software,[27] and based on measurement-setup factors, such as the solid angle and energy resolution of the detector, which cause broadening of ERDA signals. Our simulation model consists of a film layer and substrate whose compositions are assumed to be $H_bSrFeO_{2.5-b}$ and $H_c(La_{0.06}Al_{0.13}Sr_{0.14}Ta_{0.07}O_{0.6-c})$, respectively. The simulated spectra are also shown with the solid black lines in the figures. For SFO-A, a peak originating from the recoiled H atoms is seen around 1 MeV and well-reproduced with a single peak broadened by the measurement-setup-related factors only. The ERDA peak for SFO-A can, therefore, be concluded to originate from H absorbed on the film surface only. On the other hand, the H peak for SFO-B is broadened toward the lower energy side and cannot be reproduced by considering the setup-related broadening only. Given that H atoms recoiling forward from the bulk film region have lower energies than those from the surface, the additional broadening of the ERDA signal indicates that H atoms exist in the bulk film region of SFO-B due to the V_{GS}-induced protonation. The H concentration in the film region, estimated from the bulk H signal, is 0.11. For SFO-C, and the H peak is well reproduced with a single peak and by considering the setup-related broadening only. Therefore, the surface H atoms dominantly contribute to the ERDA signal while the bulk H contribution to the ERDA signal is rather small. These results support that the V_{GS}-induced electrochemical reductions lead to the protonation of $SrFeO_y$, forming $H_xSrFeO_{2.5}$ ($x \sim 0.11$).

Finally, we point out the possibility that the protonation of $SrFeO_y$ films is tied with the electrochemically induced Fe^{2+} valence state. The crystal lattice of $SrFeO_y$ ($y \geq 2.5$) can accommodate only Fe having valence states higher than +3. Accommodating Fe^{2+} in $SrFeO_y$ requires introductions of oxygen vacancies in the brownmillerite lattice framework of $SrFeO_{2.5}$. However, the brownmillerite lattice is rather rigid and the formation energies of oxygen vacancies are rather high. Alternatively, accommodating protons in the brownmillerite lattice could stabilize Fe^{2+}. This is why electrochemically reducing $SrFeO_y$ films and inducing Fe^{2+} promote their protonation. In the protonated $SrFeO_y$, the protons probably are bonded to oxygens, and the formed O–H bonds would point toward oxygen-vacancy positions, resulting in large lattice distortions. Similar O–H bonds are reported to form in hydrogenated $SrCoO_{2.5}$.[11,13] However, identifying the atomic positions of protons in $SrFeO_y$ will require further investigations.

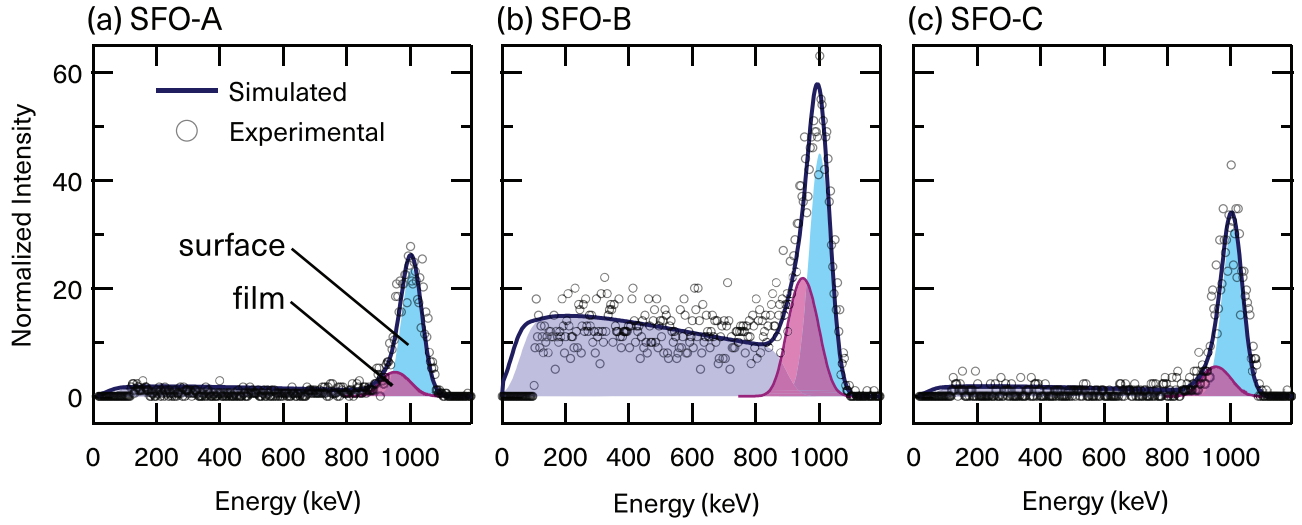

FIG. 4. Measured and simulated ERDA spectra for the (a) SFO-A, (b) SFO-B, and (c) SFO-C films. The signal originating from the hydrogen atoms absorbed on the surface and that originating from those accumulated in the films are shown with cyan and pink, respectively. The background signals colored with purple possibly arise from hydrogen in Nafion left on the films' surfaces and from hydrogen atoms diffused in substrates.

In summary, we show that by utilizing the proton-conducting solid electrolyte Nafion as a gate insulator in electric-field-effect transistor structures, the structural and transport properties of oxygen-deficient perovskite $SrFeO_y$ films can be electrochemically controlled. Furthermore, electrochemical reductions promote the protonation of the $SrFeO_y$ films and result in the formation of the proton-containing oxide $H_xSrFeO_{2.5}$ ($x \sim 0.11$). Our results indicate the usefulness of the proton-conducting solid electrolyte for electrochemically controlling transition metal oxides and for exploring proton-containing oxides.

This work was partly supported by Grants-in-Aid for Scientific Research (Nos. 19H05816, 19H05823, 20H05293, and 21H01810) and the International Collaborative Research Program of the Institute for Chemical Research in Kyoto University from the Ministry of Education, Culture, Sports, Science and Technology (MEXT) of Japan. This work was also supported by the Japan Society for the Promotion of Science Core-to-Core Program (A) Advanced Research Networks.

AUTHOR DECLARATIONS

Conflict of Interest

The authors have no conflicts to disclose.

DATA AVAILABILITY

The data that support the findings of this study are available from the corresponding author upon reasonable request.

REFERENCES

[1]M. Imada, A. Fujimori, and Y. Tokura, Rev. Mod. Phys. **70**, 1039 (1998).
[2]T. Tsuchiya, K. Terabe, M. Ochi, T. Higuchi, M. Osada, Y. Yamashita, S. Ueda, and M. Aono, ACS Nano **10**, 1655 (2016).
[3]H. Ohta, Y. Sato, T. Kato, S. Kim, K. Nomura, Y. Ikuhara, and H. Hosono, Nat. Commun. **1**, 118 (2010).
[4]Z. Li, S. Shen, Z. Tian, K. Hwangbo, M. Wang, Y. Wang, F. M. Bartram, L. He, Y. Lyu, Y. Dong, G. Wan, H. Li, N. Lu, J. Zang, H. Zhou, E. Arenholz, Q. He, L. Yang, W. Luo, and P. Yu, Nat. Commun. **11**, 184 (2020).
[5]M. Jo, H. J. Lee, C. Oh, H. Yoon, J. Y. Jo, and J. Son, Adv. Funct. Mater. **28**, 1802003 (2018).
[6]K. Shibuya and A. Sawa, Adv. Electron. Mater. **2**, 1500131 (2016).
[7]J.-T. Yang, C. Ge, J.-Y. Du, H.-Y. Huang, M. He, C. Wang, H.-B. Lu, G.-Z. Yang, and K.-J. Jin, Adv. Mater. **30**, 1801548 (2018).
[8]M. Wang, X. Sui, Y. Wang, Y.-H. Juan, Y. Lyu, H. Peng, T. Huang, S. Shen, C. Guo, J. Zhang, Z. Li, H.-B. Li, N. Lu, A. T. N'Diaye, E. Arenholz, S. Zhou, Q. He, Y.-H. Chu, W. Duan, and P. Yu, Adv. Mater. **31**, 1900458 (2019).
[9]J. Tian, H. Wu, Z. Fan, Y. Zhang, S. J. Pennycook, D. Zheng, Z. Tan, H. Guo, P. Yu, X. Lu, G. Zhou, X. Gao, and J. Liu, Adv. Mater. **31**, 1903679 (2019).
[10]C. Ge, C. Liu, Q. Zhou, Q. Zhang, J. Du, J. Li, C. Wang, L. Gu, G. Yang, and K. Jin, Adv. Mater. **31**, 1900379 (2019).
[11]N. Lu, P. Zhang, Q. Zhang, R. Qiao, Q. He, H.-B. Li, Y. Wang, J. Guo, D. Zhang, Z. Duan, Z. Li, M. Wang, S. Yang, M. Yan, E. Arenholz, S. Zhou, W. Yang, L. Gu, C.-W. Nan, J. Wu, Y. Tokura, and P. Yu, Nature **546**, 124 (2017).
[12]M. Wang, S. Shen, J. Ni, N. Lu, Z. Li, H.-B. Li, S. Yang, T. Chen, J. Guo, Y. Wang, H. Xiang, and P. Yu, Adv. Mater. **29**, 1703628 (2017).
[13]H.-B. Li, F. Lou, Y. Wang, Y. Zhang, Q. Zhang, D. Wu, Z. Li, M. Wang, T. Huang, Y. Lyu, J. Guo, T. Chen, Y. Wu, E. Arenholz, N. Lu, N. Wang, Q. He, L. Gu, J. Zhu, C.-W. Nan, X. Zhong, H. Xiang, and P. Yu, Adv. Sci. **6**, 1901432 (2019).
[14]J. B. MacChesney, R. C. Sherwood, and J. F. Potter, J. Chem. Phys. **43**, 1907 (1965).
[15]Y. Takeda, K. Kanno, T. Takada, O. Yamamoto, M. Takano, N. Nakayama, and Y. Bando, J. Solid State Chem. **63**, 237 (1986).
[16]J. P. Hodges, S. Short, J. D. Jorgensen, X. Xiong, B. Dabrowski, S. M. Mini, and C. W. Kimball, J. Solid State Chem. **151**, 190 (2000).
[17]E. K. Hemery, G. V. M. Williams, and H. J. Trodahl, Phys. Rev. B **75**, 092403 (2007).
[18]G. V. M. Williams, E. K. Hemery, and D. McCann, Phys. Rev. B **79**, 024412 (2009).
[19]M. Reehuis, C. Ulrich, A. Maljuk, C. Niedermayer, B. Ouladdiaf, A. Hoser, T. Hofmann, and B. Keimer, Phys. Rev. B **85**, 184109 (2012).
[20]K. Matsumoto, D. Kan, N. Ichikawa, S. Hosokawa, H. Kageyama, and Y. Shimakawa, Chem. Lett. **42**, 732 (2013).
[21]K. Hirai, D. Kan, N. Ichikawa, K. Mibu, Y. Yoda, M. Andreeva, and Y. Shimakawa, Sci. Rep. **5**, 7894 (2015).
[22]M. Schmidt and S. J. Campbell, J. Solid State Chem. **156**, 292 (2001).
[23]P. Adler, A. Lebon, V. Damljanović, C. Ulrich, C. Bernhard, A. V. Boris, A. Maljuk, C. T. Lin, and B. Keimer, Phys. Rev. B **73**, 094451 (2006).
[24]A. Khare, D. Shin, T. S. Yoo, M. Kim, T. D. Kang, J. Lee, S. Roh, I.-H. Jung, J. Hwang, S. W. Kim, T. W. Noh, H. Ohta, and W. S. Choi, Adv. Mater. **29**, 1606566 (2017).
[25]A. Khare, J. Lee, J. Park, G.-Y. Kim, S.-Y. Choi, T. Katase, S. Roh, T. S. Yoo, J. Hwang, H. Ohta, J. Son, and W. S. Choi, ACS Appl. Mater. Interfaces **10**, 4831 (2018).
[26]H. Yamada, M. Kawasaki, and Y. Tokura, Appl. Phys. Lett. **80**, 622 (2002).
[27]M. Mayer, "SIMNRA user's guide," Report No. IPP 9/113 (Max-Planck-Institut für Plasmaphysik, Garching, Germany, 1997).